Pergamon

Geochimica et Cosmochimica Acta, Vol. 68, No. 2, pp. 239–251, 2004
Copyright © 2004 Elsevier Ltd
Printed in the USA. All rights reserved
0016-7037/04 $30.00 + .00

doi:10.1016/S0016-7037(03)00420-4

Modeling the surface complexation of calcium at the rutile-water interface to 250°C

MOIRA K. RIDLEY,[1,*] MICHAEL L. MACHESKY,[2] DAVID J. WESOLOWSKI,[3] and DONALD A. PALMER[3]

[1]Texas Tech University, Department of Geosciences, P.O. Box 41053, Lubbock, TX 79409-1053, USA
[2]Illinois State Water Survey, 2204 Griffith Drive, Champaign, IL 61820-7495, USA
[3]Chemical Sciences Division, Oak Ridge National Laboratory, P.O. Box 2008, MS 6110, Oak Ridge, TN 37831-6110, USA

(*Received December* 20, 2002; *accepted in revised form June* 16, 2003)

Abstract—The adsorption behavior of metal-(hydr)oxide surfaces can be described and rationalized using a variety of surface complexation models. However, these models do not uniquely describe experimental data unless some additional insight into actual binding mechanisms for a given system is available. This paper presents the results of applying the MUlti SIte Complexation or MUSIC model, coupled with a Stern-based three layer description of the electric double layer, to Ca^{2+} adsorption data on rutile surfaces from 25 to 250°C in 0.03 and 0.30 *m* NaCl background electrolyte. Model results reveal that the tetradentate adsorption configuration found for Sr^{2+} adsorbed on the rutile (110) surface in the *in situ* X-ray standing wave experiments of Fenter et al. (2000) provides a good fit to all Ca^{2+} adsorption data. Furthermore, it is also shown that equally good fits result from other plausible adsorption complexes, including various monodentate and bidentate adsorption configurations. These results amply demonstrate the utility of *in situ* spectroscopic data to constrain surface complexation modeling, and the ability of the MUSIC model approach to accommodate this spectroscopic information. Moreover, this is the first use of any surface complexation model to describe multivalent ion adsorption systematically into the hydrothermal regime. *Copyright © 2004 Elsevier Ltd*

1. INTRODUCTION

The fundamental importance of chemical interactions at mineral-water interfaces in many disciplines has lead to considerable interest in characterizing this interface region, both theoretically and experimentally. Specifically, ion adsorption phenomena and the development of mineral surface charge have been studied frequently as a function of pH, at the macroscopic scale. The resulting data have been described by various surface complexation models, which differ in their formulation of the adsorption reactions and their distribution of ionic species across the interface region. The distribution of ionic species at the solid-solution interface is generally referred to as the Electric Double Layer (EDL). Although thermodynamically correct, surface complexation models are limited in other ways. For example, some models neglect molecular information concerning the structure of the mineral face; however, ion adsorption is strongly dependent on the type and number of surface sites available. In addition, our understanding of the EDL and the surface speciation of adsorbed ions has been hindered by a lack of quantitative molecular-scale experimental data. It has, therefore, been common practice to fit hypothetical surface species, and use various capacitance values to account for the electrostatic effects associated with ion adsorption on mineral surfaces.

More recently, the Multi Site Complexation (MUSIC) model has been developed (Hiemstra et al., 1989, 1996), which explicitly considers the various types of surface hydroxyl groups known to exist on mineral surfaces. Moreover, X-ray techniques, such as in situ small-period X-ray standing waves (Fenter et al., 2000; Bedzyk and Cheng, 2002) and grazing-incidence X-ray absorption (GI-XAF) spectroscopy (Towle et al., 1999a, 1999b; Waychunas, 2002), can now provide truly quantitative and detailed molecular-scale data on the structure and local geometry of adsorbed species.

Within the MUSIC model approach it is possible to rationalize and describe macroscopic ion-adsorption data within a mechanistically-accurate, thermodynamically-rigorous framework that is firmly based on crystallographic and molecular-scale information. Several previous studies involving cation adsorption on metal oxide surfaces have demonstrated the ability of the MUSIC model to directly accommodate in situ spectroscopic information, albeit within the 1-p*K* approximation and only at room temperature. Venema et al. (1996) and Boily et al. (1999) were able to fit adsorption and proton stoichiometric data for Cd^{2+} adsorption by goethite utilizing EXAFS determined Cd^{2+} adsorption geometries found by Spadini et al. (1994). Similarly, Rietra et al. (2001) were able to fit data for the adsorption of Ca^{2+} by goethite, by assuming an adsorption geometry analogous to the Sr^{2+} surface complexes identified by EXAFS (Axe et al., 1998; Collins et al., 1998; Sahai et al., 2000). Hayes and Katz (1996) and Brown et al. (1999) utilized X-ray absorption spectroscopy results to constrain a 2-p*K* triple layer model fit of Co^{2+} adsorption by Al_2O_3. The best model fits involved the adsorption of both monomeric and multimeric Co^{2+} species, as well as the surface precipitation of $Co(OH)_2$.

Surface complexation models have rarely been utilized at other than room temperatures. This is in part due to the lack of experimental adsorption data available over a wide temperature range. Sverjensky and Sahai (1998) and Kulik (2000) have provided generalized frameworks to estimate surface protonation enthalpies within the context of the 2-p*K* triple layer surface complexation model, and Sahai (2000) has extended this approach to estimating adsorption enthalpies for monova-

* Author to whom correspondence should be addressed (moira.ridley@ttu.edu).

lent electrolyte ions. A few investigations have also applied surface complexation models to specific variable temperature adsorption data. Angrove et al. (1999) investigated the adsorption of Cd^{2+} and Co^{2+} by goethite between 10 and 70°C, and utilized the 2-p*K* constant capacitance model to interpret the results. Adsorption of these cations increased with temperature and this was reflected in the endothermic adsorption enthalpies obtained from modeling. The 2-p*K* constant capacitance surface complexation model was also used by Karasyova et al. (1999) in their study of Sr^{2+} adsorption by hematite between 25 and 75°C. The increased Sr^{2+} adsorption with increasing temperature was rationalized with an increase in the Sr^{2+} binding constants and a decrease in best-fit capacitance values. Pivovarov (2001) studied the adsorption of Cd^{2+} by hematite between 25 and 100°C and used a three-plane constant capacitance model to interpret the results. Model derived adsorption enthalpies and entropies were both positive indicating that the adsorption process was entropy driven.

The most extensive set of high temperature adsorption data exists for rutile, from stirred hydrogen electrode concentration cell measurements. These studies have dealt primarily with potentiometric titration data for rutile in NaCl electrolyte solutions from 10 to 250°C (Machesky et al., 1994, 1998; Ridley et al., 2002a). Moreover, these data enabled Machesky et al. (2001) to extend the MUSIC model approach beyond room temperature.

Ridley et al. (1999) investigated the adsorption of Ca^{2+} by rutile in the presence of NaCl background electrolyte between 25 and 250°C. The principal results were that Ca^{2+} adsorption increased systematically with increasing temperature, 0.30-*m* NaCl suppressed adsorption relative to 0.03-*m* NaCl, and the proton stoichiometry (moles H^+ released/moles Ca^{2+} adsorbed) remained relatively constant with increasing temperature. The relatively constant proton stoichiometry led Ridley et al. (1999) to suggest that the chemical and/or electrostatic factors governing Ca^{2+} adsorption did not change significantly with increasing temperature.

In this study we present the results of modeling the Ca^{2+} adsorption data from Ridley et al. (1999) within the context of the temperature compensated MUSIC model approach of Machesky et al. (2001) coupled with a Stern-based description of the EDL structure. We also make the plausible assumption that the tetradentate, inner sphere, adsorption geometry found by Fenter et al. (2000) for Sr^{2+} adsorption on the rutile (110) surface constitutes the primary mode of Ca^{2+} adsorption by our rutile powder as well. This assumption is justified by preliminary studies of Sr^{2+} adsorption on the same rutile powders in NaCl, Sodium-Trifluomethanesulphonate (NaTr) and RbCl media (Ridley et al., 2002b, 2002c), which demonstrate very similar behavior of Ca^{2+} and Sr^{2+}. This adsorption complex can be modeled explicitly within the MUSIC model framework. Finally, we compare the model results of this "actual" adsorption complex with results from other conceivable adsorption geometries, and with the 1-p*K* and CD-MUSIC model approaches (Hiemstra and van Riemskijk, 1996). It is demonstrated that the in situ spectroscopic information is necessary to uniquely describe Ca^{2+} adsorption by rutile, that the MUSIC model can directly and successfully accommodate this spectroscopic information, and that the tetradentate adsorption complex observed at room temperature also adequately describes Ca^{2+} adsorption to 250°C. To our knowledge, this is the first study to systematically model the adsorption of a multivalent ion over such a wide temperature range.

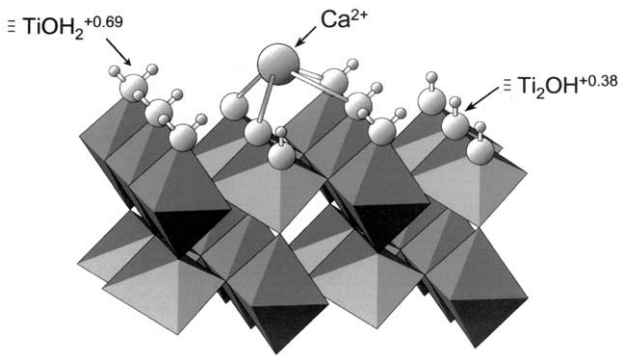

Fig. 1. Negatively-charged rutile (110) surface with Ca^{2+} binding in a tetradentate configuration, involving two terminal ($\equiv TiOH^{-0.31}$) and two bridging ($\equiv Ti_2O^{-0.62}$) surface groups.

2. MODELING BACKGROUND

The initial step in specific-ion adsorption modeling is to describe the pH-dependent primary charge on the mineral of interest. The simplest representation of proton induced surface charge on metal-(hydr)oxide phases is the "1-p*K* model" (Bolt and van Reimsdijk, 1982; Gibb and Koopal, 1990), which can also be considered the simplest version of the MUSIC model (Hiemstra et al., 1989, 1996). The full MUSIC model specifically considers the crystal structure of minerals, including types, concentrations, and bonding geometries of the ≡S-OH surface sites present on metal-(hydr)oxide phases. With this information the MUSIC model predicts the proton binding constants for a variety of terminal oxygen sites, from an independent empirical model based on the Pauling bond-valence principle (Hiemstra et al., 1989). In the Charge Distribution extension of the MUSIC model (CD-MUSIC) the charge of adsorbed ions is distributed between the surface and Stern layer adsorption planes (Hiemstra and van Riemsdijk, 1996; Venema et al., 1996).

2.1. MUSIC Model Protonation Reactions

The formulation of the temperature-compensated MUSIC model and its application to rutile has been discussed in detail by Machesky et al. (2001). Briefly, application of the MUSIC model requires knowledge of the predominant external crystallographic planes of rutile, along with the types, concentrations, and bonding geometries of the Ti-O groups present on these faces. Jones and Hockey (1971) have suggested that the predominant crystallographic planes of many powdered rutile samples are the (110), (100), and (101) faces, in a ratio of ~0.6:0.2:0.2. This is approximately true for our powdered rutile since the (110) surface clearly predominates (Ridley et al., 2002a). For this representation of the rutile surface, two independent surface groups predominate: singly coordinated (or terminal) hydroxyls and doubly coordinated (or bridging) surface oxygen atoms (Fig. 1), in an ideal 1:1 ratio. These surface sites and their protonation reactions are represented by

Table 1. Relevant MUSIC-Basic Stern model constants and variable parameter values from Machesky et al. (2001).

T (°C)	'A'	1/2 pK_w	log K_{H1}	log K_{H2}	pH_{znpc}	pH_{ppzc}	C_s (F · m^{-2})	SD_C	K_M	SD_{KM}	K_A	SD_{KA}	MSC
25	21.700	6.996	6.722	4.763	5.4	5.402	2.065	0.080	0.058	0.012	0.0020	0.003	4.52
50	20.490	6.635	6.347	4.498	5.1	5.117	2.051	0.064	0.068	0.011	0.0025	0.002	5.02
100	18.713	6.131	5.796	4.108	4.7	4.695	2.057	0.070	0.080	0.011	0.021	0.005	4.86
150	17.647	5.820	5.466	3.874	4.4	4.439	2.393	0.108	0.085	0.013	0.020	0.005	4.35
200	16.917	5.650	5.240	3.714	4.3	4.263	2.740	0.097	0.090	0.009	0.037	0.005	4.84
250	16.452	5.598	5.096	3.612	4.2	4.150	3.332	0.137	0.182	0.018	0.073	0.009	4.62

'A' = a temperature-dependent constant; 1/2 pK_w = one-half the dissociation constant of water; log K_{Hn} = surface site protonation constants; pH_{znpc} = experimental value for the pH of zero net proton charge; pH_{ppzc} = pH value of the predicted pristine point of zero charge; C_S = capacitance value of the Stern Layer; SD_C = Standard Deviation of the Stern Layer capacitance value; K_M and K_A = cation and anion binding constants, respectively; SD_{KM} and SD_{KA} = Standard Deviation of the cation and anion binding constants, respectively; and MSC = Model Selection Criteria. $K_{H1} : K_{H2} = 0.402 : 0.598$.

$$\equiv TiOH^{-0.31} + H^+ = \equiv TiOH_2^{+0.69}\, K_{H1} \quad (1)$$

$$\equiv Ti_2O^{-0.62} + H^+ = \equiv Ti_2OH^{+0.38}\, K_{H2} \quad (2)$$

The protonation constants for these reactions, the corresponding pH values at the pristine point of zero charge (pH_{ppzc}) and the experimental pH_{znpc} values, as discussed in greater detail by Machesky et al. (2001) are given in Table 1. Machesky et al. (2001) assumed the Ti-O bond lengths of these groups were 1.94 Å, and that the total surface site concentration was 20.8 μmol · m^{-2}. With these values and assuming a ratio of 0.402: 0.598 for the singly to doubly coordinated surface hydroxyl groups, model predicted and experimentally determined pH_{znpc} values agreed to within 0.06 pH units between 25 and 250°C. This same surface scheme was used in this study.

2.2. One-p*K* Model Protonation Reactions

In the 1-p*K* model surface sites are represented by a single terminal charge-determining site, which may exchange protons with the solution. For rutile, this is given by

$$\equiv Ti\text{-}OH^{-0.50} + H^+ = \equiv Ti\text{-}OH_2^{+0.50} \quad (3)$$

where $\equiv Ti\text{-}OH^{-0.50}$ and $\equiv Ti\text{-}OH_2^{+0.50}$ are deprotonated and protonated ≡Ti-OH groups, respectively. The equilibrium constant for this reaction is

$$K_H = [\equiv Ti\text{-}OH_2^{+0.50}]/([\equiv Ti\text{-}OH^{-0.50}] \times \{H^+\}_b \exp[-zF\Psi/RT]) \quad (4)$$

Where [] = concentration, $\{H^+\}_b$ = bulk hydrogen ion activity (10^{-pH}), z = hydrogen ion charge, F = Faraday constant, Ψ = potential at the proton adsorption plane, R = gas constant, and T = temperature in kelvins. The protonation constant (log K_H) describing the surface hydroxyl group ionization can be equated with the measured pH of zero net proton charge, pH_{znpc}. Accordingly, at the pH_{znpc}, $[\equiv Ti\text{-}OH^{-0.50}] = [\equiv Ti\text{-}OH_2^{+0.50}]$ and $\Psi = 0$; therefore, log $K_H = pH_{znpc}$. For additional details see Bolt and van Reimsdijk (1982), Gibb and Koopal (1990), Machesky et al. (1998), and Ridley et al. (2002a).

2.3. Surface Complexation Modeling

Surface complexation modeling of proton adsorption data combines chemical descriptions of the surface group behavior with coulombic or electrostatic corrections based on an assumed EDL structure. In the present study the EDL structure utilized by Machesky et al. (2001) was applied, and is summarized here briefly. In addition to using the temperature-compensated MUSIC model, Machesky et al. (2001) assumed a Basic Stern layer description of the EDL structure when fitting rutile proton adsorption data. A sketch of the EDL structure is given in Figure 2A., and from the surface outward comprises, protonation at the mineral surface (defined by K_{H1} and K_{H2}), specific cation and anion binding of the electrolyte ions at the Stern layer (defined by K_M and K_A), and the diffuse layer. In this model, the electrolyte counterions are assigned to the same Stern plane, with the proton charge asymmetry accounted for by the relative magnitudes of the counterion binding constants (cation constants greater than anion constants). Furthermore, the counterion binding constants were held equal for both types of rutile surface sites considered. Mean molal stoichiometric activity coefficients for NaCl were taken from Pitzer et al. (1984), and it was assumed that $\gamma_{Na+} = \gamma_{Cl-} = \gamma_{\pm NaCl}$. The capacitance value (F · m^{-2}) of the Stern layer (C_S) was a fitting parameter used in conjunction with the Guoy-Chapman theory to determine the associated surface (Ψ_0), Stern layer (Ψ_M and Ψ_A) and diffuse layer (Ψ_D) potentials. Under the Basic Stern approach, $\Psi_M = \Psi_A = \Psi_D$. The fitting parameters of Machesky et al. (2001) are summarized in Table 1.

Tables 1 to 4 include standard deviations (or confidence intervals)for the best-fit parameter values (SD) and model selection criterion (MSC) values. The SD values were estimated separately for each parameter (i.e., no correlation between the fitted parameters); moreover, it was assumed that the parameters behaved linearly near the best-fit solution. The MSC value is a normalized inverse form of the Akaike Information Criterion (Akaike, 1976). It is a measure of the goodness of fit of the model, with larger values signifying better fits.

The proton adsorption data of Machesky et al. (2001) were refitted here, using the 1-p*K* model and the Basic Stern layer description of the EDL structure as described above. This is a simplification of the 1-p*K*, three plane model used in Machesky et al. (1998). In this description of proton adsorption at a mineral surface, a single protonation constant, K_H, replaces K_{H1} and K_{H2} in Figure 2. The fitted parameters for the 1-p*K* model are given in Table 2. MSC values are similar to those obtained by Machesky et al. (2001) (Table 1), signifying a similar quality of fit.

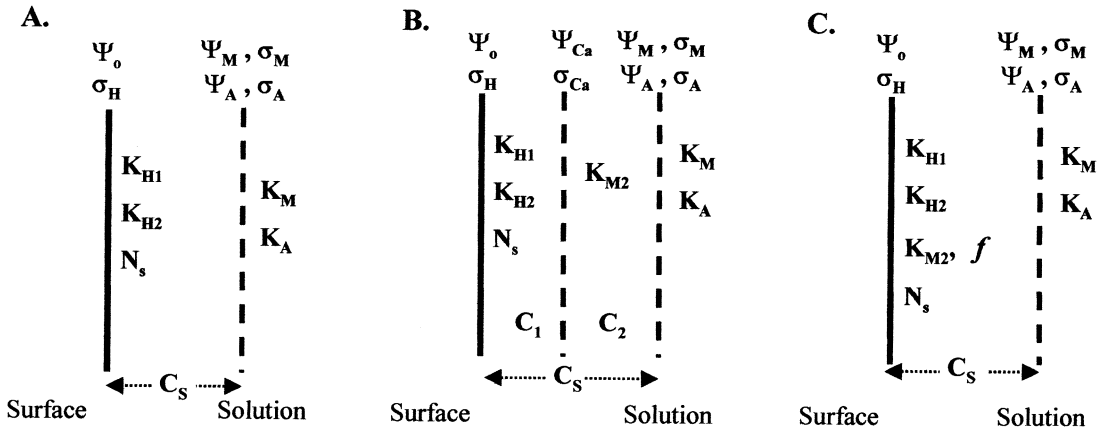

Fig. 2. Schematic representations of the EDL structure combined with the MUSIC and CD-MUSIC models. The notation represents protonation (K_{Hn}), cation (K_M), anion (K_A) and calcium (K_{M2}) binding constants; Ψ_n and σ_n are the potential and charge at the binding planes, respectively; C_S is the capacitance value of the Stern Layer; N_S is the surface site concentration, fixed at 20.8 μmol $\cdot$ m^{-2} (12.5 sites $\cdot$ nm^{-2}); and f is the charge distribution factor for calcium. In sketch A the MUSIC model is combined with a Basic Stern layer description of the EDL for the interaction of NaCl with the rutile surface. Sketch B shows a Three-layer representation of the EDL combined with the MUSIC model, where Ca^{2+} is bound immediately adjacent to the rutile surface. Sketch C combines the CD-MUSIC model with a Basic Stern layer description of the EDL. In this representation, the charge of the Ca ion is distributed between the rutile surface and inner-most Stern plane.

3. CALCIUM ADSORPTION MODELING

Two independent sets of sorption data were obtained by Ridley et al. (1999). One set, referred to as "surface charge" isotherms, were obtained by equating the "excess" or "missing" protons in solution, in micromoles of H^+ per square meter of mineral surface with the proton-induced surface charge via the relation, $\sigma_H \equiv -$F(micromoles excess H^+)/m^2. The other set, referred to as "pH sorption edge isotherms," consisted of similar titrations during which samples were removed for analysis of the total dissolved Ca concentration. At each temperature studied, four separate sets of surface charge and pH sorption isotherms, in 0.03 and 0.30 molal NaCl with 0.001-*m* initial Ca^{2+} were fit simultaneously. All model parameters determined from fitting the NaCl only proton charge data were fixed at those values given in Tables 1 and 2 for modeling the Ca^{2+} adsorption data. The EDL structure was expanded from the Basic Stern to a three-layer model (Fig. 2B), with a Ca-binding plane positioned immediately adjacent to the rutile surface. This three-plane EDL structure is consistent with the results of Fenter et al. (2000) who found that Rb^+ was positioned higher above the rutile (110) surface than Sr^{2+}. Consequently, the only variable fitting parameters were a Ca^{2+} binding constant, K_{M2}, and the capacitance value (F $\cdot$ m^{-2}) for the Ca-binding plane, C_1. The Stern layer capacitance values are related by

$$1/C_s = 1/C_1 + 1/C_2 \quad (5)$$

where C_S = the Stern layer capacitance as determined from fitting the NaCl only data (Tables 1 and 2), and C_2 = the capacitance value of the outer counterion binding plane and is determined by difference. Furthermore, a small offset value was applied to each Ca-adsorption isotherm. These offset values set the starting σ_H of the Ca-adsorption isotherms equal to the surface charge value at the appropriate pH of the corresponding protonation isotherm in NaCl media without Ca^{2+} present. These small offset corrections reflect slight differences in the starting EMF potentials of the individual titrations, and are not due to significant Ca^{2+} adsorption since the corresponding adsorption pH edge data indicate that Ca^{2+} adsorption is insignificant at the start of all titrations. In all modeling efforts, the activity coefficient for Ca^{2+} was assumed equal to the activity coefficient for the Na^+ and Cl^- counterions to the fourth power, such that $\gamma_{Ca2+} = (\gamma_{\pm NaCl})^4$. This square of charge approximation, originally due to Meissner and Kusik (1972) was found to be reasonably accurate by Holmes et al.

Table 2. Model constants and variable parameter values for the data of Machesky et al. (2001) refitted using a 1-p*K* - Basic Stern model.

T (°C)	pH_{znpc}	C_s (F $\cdot$ m^{-2})	SD_C	K_M	SD_{KM}	K_A	SD_{KA}	MSC
25	5.4	1.778	0.043	0.041	0.008	0.0020	0.003	5.09
50	5.1	1.855	0.036	0.048	0.007	0.0025	0.002	5.79
100	4.7	1.930	0.042	0.057	0.007	0.021	0.005	5.40
150	4.4	2.046	0.075	0.084	0.015	0.020	0.005	4.41
200	4.3	2.330	0.066	0.092	0.011	0.037	0.005	5.00

$K_H = 10^{-pHznpc}$; C_S = capacitance value of the Stern Layer; K_M and K_A = cation and anion binding constants, respectively; SD_n = Standard Deviation of the relevant parameter; and MSC = Model Selection Criteria.

Table 3. MUSIC-Basic Stern model constants and variable parameter values for the adsorption of Ca^{2+} onto rutile in a tetradentate configuration.

T (°C)	pH_{znpc}	log K_{TET}	$SD_{logKTET}$	C_1 (F · m^{-2})	SD_C	MSC
25	5.4	17.60	0.13	3.93	0.23	5.48
50	5.1	17.77	0.17	4.60	0.37	4.64
100	4.7	18.20	0.13	5.00	0.51	5.19
150	4.4	18.75	0.45	5.25	0.19	6.43
200	4.3	19.35	0.10	5.60	0.61	5.36
250	4.2	19.99	0.22	6.52	1.38	3.37

pH_{znpc} = experimental value for the pH of zero net proton charge; log K_{TET} = Ca^{2+} binding constant in a tetradentate configuration; C_1 = capacitance value for the Ca-binding plane; SD_n = Standard Deviation of the relevant parameter; and MSC = Model Selection Criteria.

(1994) in predicting mean activity coefficients of $CaCl_2^0$ to 1 *m*. Free Ca^{2+} was assumed to be the only calcium species adsorbed, and no corrections were made for either hydrolysis or Cl^- complexation of the total calcium remaining in solution at any experimental condition.

3.1. Application of the MUSIC Model

The actual or true Ca^{2+} adsorption configuration is assumed to be tetradentate by analogy with the X-ray standing wave results for Sr^{2+} adsorption on the rutile (110) surface (Fenter et al., 2000) (Fig. 1). The same teteradentate adsorption configuration is assumed for the rutile (100) surface, because both (100) and (110) surfaces have the same surface site geometries. The MUSIC model representation of this reaction is

$$2(\equiv TiOH^{-0.31}) + 2(\equiv Ti_2O^{-0.62}) + Ca^{2+} = [(\equiv TiOH^{-0.31})_2(\equiv Ti_2O^{-0.62})_2] - Ca^{2+} \quad (6)$$

However, had this in situ spectroscopic information not been available, various other surface complexation reactions would have been equally plausible. The primary mono- and bidentate adsorption possibilities are

$$\text{monodentate } \equiv TiOH^{-0.31} + Ca^{2+} = [\equiv TiOH^{-0.31}] - Ca^{2+} \quad (7)$$

$$\equiv Ti_2O^{-0.62} + Ca^{2+} = [\equiv Ti_2O^{-0.62}] - Ca^{2+} \quad (8)$$

$$\text{bidentate } 2(\equiv TiOH^{-0.31}) + Ca^{2+} = [(\equiv TiOH^{-0.31})_2] - Ca^{2+} \quad (9)$$

$$2(\equiv Ti_2O^{-0.62}) + Ca^{2+} = [(\equiv Ti_2O^{-0.62})_2] - Ca^{2+} \quad (10)$$

$$\equiv TiOH^{-0.31} + \equiv Ti_2O^{-0.62} + Ca^{2+} = [(\equiv TiOH^{-0.31})(\equiv Ti_2O^{-0.62})] - Ca^{2+} \quad (11)$$

Model parameter values for tetradentate adsorption of Ca^{2+} onto rutile are as follows. The surface site concentration is given by

$$N_s = [TiOH^{z_1}] + [TiOH_2^{(z_1+z_H)}] + [TiOH^{z_1} - M^+] + [TiOH_2^{(z_1+z_H)} - A^-] + [Ti_2O^{z_2}] + [Ti_2OH^{(z_2+z_H)}] + [Ti_2O^{z_2} - M^+] + [Ti_2OH^{(z_2+z_H)} - A^-] + [(TiOH^{z_1})_2(Ti_2O^{z_2})_2 - Ca^{2+}] \quad (12)$$

where M^+ and A^- represent the outer Stern layer electrolyte cations and anions, respectively, and $[(TiOH^{z_1})_2(Ti_2O^{z_2})_2 - Ca^{2+}]$ represents the tetradentate Ca-adsorption configuration. Ion charges are $z_1 = -0.31$ and $z_2 = -0.62$ for the terminal and bridged surface hydroxyl groups, respectively, and z_H = hydrogen ion charge (+1). All parameters for the surface protonation constants and electrolyte ion binding constants are identical to those given in Machesky et al. (2001). The tetradentate binding constant for reaction 6 was a fitting parameter and is defined as

$$K_{TET} = [(\equiv TiOH^{-0.31})_2(\equiv Ti_2O^{-0.62})_2 - Ca^{2+}]/\{[\equiv TiOH^{-0.31}]^2[\equiv Ti_2O^{-0.62}]^2[Ca^{2+}]_b(\gamma_{Ca}) \exp(-z_{Ca}F\Psi_{Ca}/RT)\} \quad (13)$$

where $[Ca^{2+}]_b$ = free calcium concentration (molal) in the bulk solution, γ_{Ca} = molal stoichiometric activity coefficient of Ca^{2+} at a given ionic strength and temperature, as defined

Table 4. Adsorption constants and variable parameter values for the adsorption of Ca^{2+} onto rutile.

Configuration	Structure	log K_{Ca}	SD_{logKCa}	C_1 (F · m^{-2})	SD_{C1}	f	SD_f	MSC
Tetradentate	$[(\equiv Ti\text{-}OH^{-0.31})_2(\equiv Ti_2\text{-}O^{-0.62})_2] - Ca^{2+}$	17.596	0.129	3.930	0.229			5.48
Bidentate	$[(\equiv Ti\text{-}OH^{-0.31})(\equiv Ti_2\text{-}O^{-0.62})] - Ca^{2+}$	6.288	0.110	3.983	0.218			5.77
Bidentate	$[(\equiv Ti_2\text{-}O^{-0.62})_2] - Ca^{2+}$	4.796	0.155	6.128	0.523			5.66
Bidentate	$[(\equiv Ti\text{-}OH^{-0.31})_2] - Ca^{2+}$	7.726	0.119	3.566	0.178			5.64
Monodentate	$[\equiv Ti_2\text{-}O^{-0.62}] - Ca^{2+}$	–0.170	0.115	5.920	0.482			5.67
Monodentate	$[\equiv Ti\text{-}OH^{-0.31}] - Ca^{2+}$	1.304	0.110	4.011	0.219			5.77
Tetradentate, 1 pK	$[(\equiv Ti\text{-}OH^{-0.50})_4] - Ca^{2+}$	16.007	0.109	3.843	0.193			5.74
Tetradentate, CD Music	$[(\equiv Ti\text{-}OH^{-0.31})_2(\equiv Ti_2\text{-}O^{-0.62})_2] - Ca^{2+}$	16.915	0.334	6.686	3.122	0.300	0.079	4.14

log K_{Ca} = Ca^{2+} binding constant; C_1 = capacitance value for the Ca-binding plane; f = the charge distribution factor for calcium in the CD-MUSIC model; SD_n = Standard Deviation of the relevant parameter; and MSC = Model Selection Criteria.

above, z_{Ca} = calcium charge (+2), and Ψ_{Ca} = potential at the inner Ca binding plane. This formulation of the tetradentate binding constant is based on the concentration of surface species (mol · m^{-2}); however, an alternate approach would be to recast the equilibrium constant in terms of dimensionless surface fractions (Venema et al., 1996).

The capacitance value (F · m^{-2}) of the Ca binding plane (C_1) was a second fitting parameter, used to determine the associated surface, inner binding plane and Stern layer potentials. These potentials can be expressed as

$$\Psi_0 = (\sigma_H/C_1) + \Psi_{M2} \quad (14)$$

$$\Psi_{M2} = (\sigma_{Ca} + \Psi_0 C_1 + \Psi_M C_2)/(C_1 + C_2) \quad (15)$$

$$\Psi_d = \Psi_M = \Psi_A = (2RT/F)\ \text{arcsinh}[-\sigma_d/(8RT\varepsilon_0\varepsilon_b I\rho_s)^{1/2}] \quad (16)$$

where ε_0 = permittivity of vacuum = 8.854×10^{-12}, ε_b = bulk dielectric constant of water at a given temperature (Archer and Wang, 1990) and ionic strength (Helgeson et al., 1981), I = stoichiometric molal ionic strength, and ρ_s = solution density which was taken from tabulated properties of NaCl solutions (Pitzer et al., 1984). The solution density term is necessary since the Gouy-Chapman theory, which is used to calculate Ψ_d above, is typically formulated in terms of molar (per unit volume) concentration units.

The charge associated with each layer is defined as follows: σ_H = net proton or surface charge,

$$\begin{aligned}\sigma_H = F\{&[TiOH_2^{(z_1+z_H)}](z_1 + z_H) \\ &+ [TiOH_2^{(z_1+z_H)} - A^-](z_1 + z_H) + [TiOH^{z_1}](z_1) \\ &+ [TiOH^{z_1} - M^+](z_1) + [Ti_2OH^{(z_2+z_H)}](z_2 + z_H) \\ &+ [Ti_2OH^{(z_2+z_H)} - A^-](z_2 + z_H) + [Ti_2O^{z_2}](z_2) \\ &+ [Ti_2O^{z_2} - M^+](z_2) + [(TiOH^{z_1})_2(Ti_2O^{z_2})_2 \\ &- Ca^{2+}][2(z_1 + z_2)]\}\end{aligned} \quad (17)$$

σ_{Ca} = charge at the Ca^{2+} binding plane (inner Stern layer),

$$\sigma_{Ca} = F\{[(TiOH^{z_1})_2(Ti_2O^{z_2})_2 - Ca^{2+}](z_{Ca})\} \quad (18)$$

σ_M = outer Stern layer cation charge (due to Na^+),

$$\sigma_M = F\{([TiOH^{z_1} - M^+] + [Ti_2O^{z_2} - M^+])(z_M)\} \quad (19)$$

σ_A = outer Stern layer anion charge (due to Cl^-),

$$\sigma_A = F\{([TiOH_2^{(z_1+z_H)} - A^-] + [Ti_2OH^{(z_2+z_H)} - A^-])(z_A)\} \quad (20)$$

σ_S = Total Stern layer charge,

$$\sigma_S = \sigma_M + \sigma_A + \sigma_{Ca} \quad (21)$$

σ_d = uncompensated or diffuse layer charge,

$$\begin{aligned}\sigma_d = -F\{&[TiOH^{z_1}](z_1) + [TiOH_2^{(z_1+z_H)}](z_1 + z_H) \\ &+ [TiOH^{z_1} - M^+](z_1 + z_M) \\ &+ [TiOH_2^{(z_1+z_H)} - A^+](z_1 + z_H + z_A) + [Ti_2O^{z_2}](z_2) \\ &+ [Ti_2OH^{(z_2+z_H)}](z_2 + z_H) \\ &+ [Ti_2O^{z_2} - M^+](z_2 + z_M) \\ &+ [Ti_2OH^{(z_2+z_H)} - A^+](z_2 + z_H + z_A) \\ &+ [(TiOH^{z_1})_2(Ti_2O^{z_2})_2 - Ca^{2+}][2(z_1 + z_2) + z_{Ca}]\}\end{aligned} \quad (22)$$

Finally, electroneutrality requires that

$$\sigma_H + \sigma_{Ca} + \sigma_M + \sigma_A + \sigma_d = 0 \quad (23)$$

Equations for modeling the other plausible mono- and bidentate adsorption configurations were identical, expect that the appropriate binding constant expression was substituted for Eqn. 13.

All surface charge and adsorption pH edge isotherm data at each temperature were fit simultaneously (typically four sets of experimental data). Model output included the variable fitting parameters, C_1 and binding constants (K_{Ca}) for the appropriate Ca-surface species, corresponding best-fit σ_H and adsorption pH edge values, MSC values, and standard deviations for the variable parameter values.

3.2. Application of the CD-MUSIC Model

The Charge Distribution (CD) variation of the MUSIC model (CD-MUSIC) was also used to fit the Ca-adsorption data (Fig. 2C). Adsorbed ions are usually considered as point charges in surface complexation models. In the typical CD-MUSIC model approach, the charge of adsorbed inner-sphere complexes is distributed between the surface and inner-most Stern planes, while adsorbed complexes at the outer Stern plane are still treated as point charges (Hiemstra and Vvan Riemsdijk, 1996; Rietra et al., 1999, 2001; Venema et al., 1996).

As applied to adsorbed Ca^{2+}, a certain fraction of the Ca^{2+} ion charge (*f*) is attributed to the surface plane, and the remaining part (1-*f*) is attributed to the inner-most Stern plane. The "actual" tetrahedral adsorption geometry was assumed, and *f* was considered to be an additional fitting parameter (in addition to C_1 and K_{TET}). Preliminary trials with *f* fixed at 0.5 yielded considerably poorer fits. An *f* value of 0.5 would be expected assuming that the inner coordination sphere of Ca^{2+} in solution contains eight water molecules, and four of these are released in forming the inner-sphere, tetradentate adsorption complex.

3.3. Application of the 1-p*K* Model

The 1-p*K* model was applied only to the tetradentate adsorption complex. The resulting adsorption reaction and binding constant are

$$4(\equiv Ti\text{-}OH^{-0.50}) + Ca^{2+} = (\equiv Ti\text{-}OH^{-0.50})_4 - Ca^{2+} \quad (24)$$

$$K_{TET\text{-}1pK} = [(\equiv TiOH^{-0.50})_4 - Ca^{2+}]/\{[\equiv TiOH^{-0.50}]^4 [Ca^{2+}]_b(\gamma_{Ca})\exp(-z_{Ca}F\Psi_{Ca}/RT)\} \quad (25)$$

As for the full MUSIC model fits, C_1 and the Ca^{2+} binding

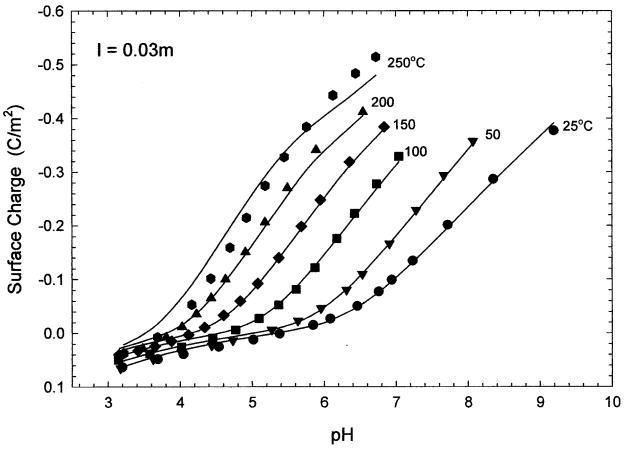

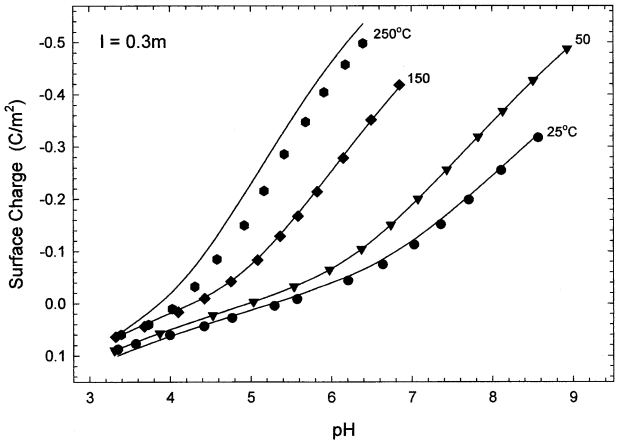

Fig. 3. MUSIC Model fits of proton charge and pH for a single tetradentate surface complex and a three-layer description of the EDL structure. Experimental data from Ridley et al. (1999) are shown as closed symbols, and the best-fit curves are shown as solid lines. All model parameter values are defined in the text and are given in Tables 1 and 3.

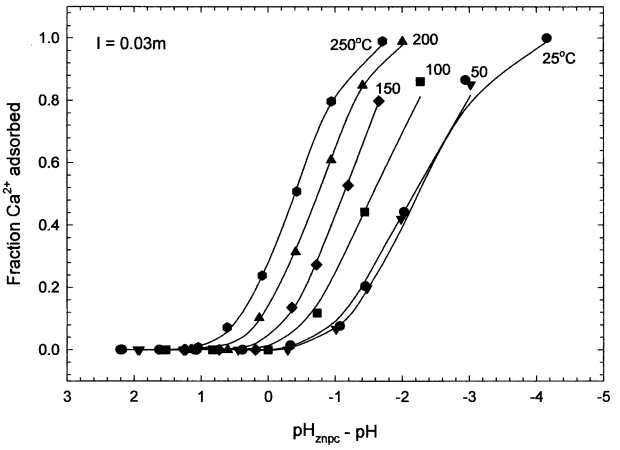

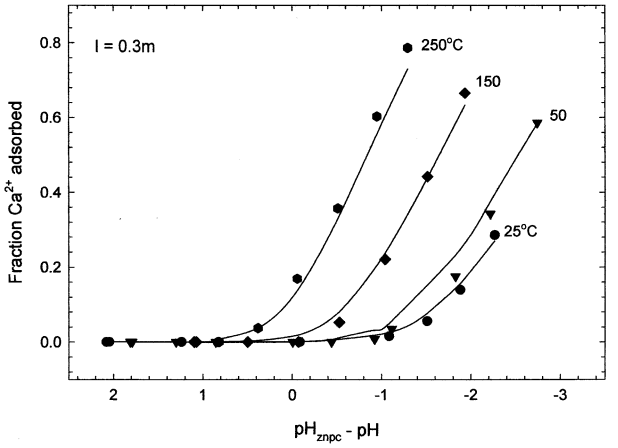

Fig. 4. MUSIC Model fits of adsorption 'pH-edge' data and (pH_{znpc}-pH) for a single tetradentate surface complex and a three layer description of the EDL structure. Experimental data from Ridley et al. (1999) are shown as closed symbols, and the best-fit curves are shown as solid lines. All model parameter values are defined in the text and are given in Tables 1 and 3.

constant (in this instance $K_{\text{TET-1pK}}$) were the only variable fitting parameters.

4. RESULTS AND DISCUSSION

4.1. MUSIC Model Fit for the Tetradentate Surface Complex

Overall, a single tetradentate surface complex coupled with a three layer description of the EDL structure provided a good description of the experimental data at all conditions. Experimental data (shown throughout as filled symbols) and best-fit curves (solid lines) for the sorption of Ca^{2+} onto rutile are shown in Figures 3 and 4 for the surface charge and adsorption edge data, respectively. The associated variable parameter, SD and MSC values are presented in Table 3.

The MSC values are similar for all temperatures, with a somewhat lower quality of fit at 250°C. From Figure 3 it is apparent that the lower MSC value at 250°C results from the predicted curves over estimating the experimental σ_H values, particularly at 0.3-*m* ionic strength; however, the model predicts the 250°C adsorption edge data (Fig. 4) satisfactorily. In an attempt to improve the fit at 250°C additional surface species were considered. Specifically, following the suggestion of Criscenti and Sverjensky (1999) hydrolyzed-Ca surface complexes and $CaCl^+$ surface species were considered. However, inclusion of these species did not improve the quality of fit at 250°C. Consequently, the specific reasons for the relatively poor fit to the 250°C data remain unknown. In any case, as pointed out by Ridley et al. (1999), the relatively constant proton stoichiometry with increasing temperature suggests that the predominant adsorption mechanism also remains constant.

Titration data were also available at 50 and 150°C in 0.30 molal NaCl, with 0.002-*m* initial Ca^{2+} (Ridley et al., 1999). These data were simply simulated with the MUSIC model parameter values presented in Tables 1 and 3. MSC values of 5.24 and 3.65 were obtained for the 50 and 150°C data, respectively. Clearly, the quality of the 50°C fit was similar to the corresponding 0.001-*m* initial Ca^{2+} data. The lower MSC value

at 150°C results from the predicted curve slightly underestimating the experimental σ_H and adsorption edge values at high pH values.

4.2. Model Fits of Alternate Surface Complexes

Model results from assuming other possible Ca^{2+} adsorption complexes at 25°C are given in Table 4 and Figure 5. With the exception of the CD-MUSIC result, MSC values for these alternate fits range between 5.64 and 5.77, compared to 5.48 for the "actual" tetradentate adsorption complex (also given in Table 4 and Fig. 5A). Consequently, only the CD-MUSIC result could be called into question on the basis of goodness-of-fit to the macroscopic adsorption data. Closer examination of the model parameter values reveals that the best-fit C_1 values for the mono- and bidentate adsorption configurations involving Ca^{2+} binding only to the Ti_2-$O^{-0.62}$ site are rather high, even for inner-sphere coordination. Similarly, the best-fit C_1 value for the CD-MUSIC fit is high. That is, these best-fit capacitance values are close to the maximum value predicted ($\sim$7) given the bare ionic radius of Ca^{2+} ($\sim$1 Å, Marcus, 1995) and a corresponding Stern layer dielectric constant equal to the bulk water value (see Eqn. 27 below). This might call into question the validity of these alternative fits relative to the other possibilities. Even so, it would not be possible to decide against the remaining alternative Ca^{2+} complexes (with MSC and C_1 values similar to the tetradentate adsorption complex) without the in situ spectroscopic information. This same ambiguity in model fits occurs at the other temperatures (50, 100, 150, 200, and 250°C) as well. Moreover, we cannot exclude the possibility that some of these alternate or other surface complexes exist on steps, kinks or other minor crystal faces of our rutile powders.

In fact, it is the combination of macroscopic adsorption data, the MUSIC model approach and corresponding in situ spectroscopic information that provides the most accurate picture of ion adsorption by metal oxide surfaces in general, and Ca^{2+} adsorption by rutile, in particular.

4.3. Temperature Dependence

The most significant trend in the best-fit parameter values associated with the tetradentate adsorption complex (Table 3) is the systematic increase in K_{TET} and C_1 with increasing temperature (Fig. 6). The systematic increase in K_{TET} is anticipated by analogy to increased ion association in solution with increasing temperature (Mesmer et al., 1988). It has been shown in this and our previous studies of rutile sorption, that the surface charge density at constant ionic strength and pH relative to the point of zero charge, increases with increasing temperature (Machesky et al., 1998; Ridley et al., 2002a), particularly for negatively charged surfaces in NaCl media. However, in addition to the coulombic attraction of dissolved ions to the fixed plane of charge at the mineral surface, sorption of an ion at an oxide surface can be viewed as a competition between bulk aqueous and surface oxygens for coordination (solvation) of the ion (James and Healy, 1972). The bulk dielectric constant of the mineral cannot change significantly with temperature, but the bulk dielectric constant of the aqueous phase decreases dramatically with increasing temperature. This alone would provide a driving force for enhanced sorption of charged species with increasing temperature, which is further enhanced or diminished by an oppositely or similarly charged surface, respectively.

The Ca^{2+} binding constants presented in Figure 6 can be fit by the equation (Murray and Cobble, 1980)

$$\log K_{TET} = -[\Delta H^\circ_{298} - 298\Delta C_p/2.303R]T^{-1} + [\Delta S^\circ_{298} - \Delta C_p(1 + \ln 298)/2.303R] + (\Delta C_p/R)\log T \quad (26)$$

where T is temperature in kelvins and ΔH°_{298}, ΔS°_{298} and ΔC_P are the standard enthalpy, entropy and heat capacity changes associated with the adsorption of Ca^{2+} onto rutile. ΔC_P is assumed to be independent of temperature. The best-fit ΔH°_{298}, ΔS°_{298} and ΔC_P values for the MUSIC model are 7.93 ± 0.54 kJ · mol^{-1}, 363.48 ± 1.71 J · K^{-1} · mol^{-1}, and 256.84 ± 6.10 J · K^{-1} · mol^{-1}, respectively. Most previous studies of ion adsorption on oxide surfaces have assumed $\Delta C_P = 0$ because of the limited temperature studied. However, the temperature dependence of log K_{TET} values shown in Figure 6 suggests that a significant positive heat capacity term is associated with the Ca^{2+} adsorption process. Machesky et al. (2001) also found positive heat capacities for proton binding at the rutile surface in NaCl media. Analysis of the thermodynamic data indicates that the adsorption reaction is slightly endothermic at 25°C and is driven by a large entropy term, which is typical of homogeneous ion association reactions in general. Furthermore, the large tetradentate binding constants and associated thermodynamic data for Ca^{2+} support the suggestion of Towle et al. (1999b), that there is a strong Gibbs energy driving force for complexed metal ions to be maximally coordinated by surface O atoms, given the steric and bonding constraints imposed by the local arrangements of the surface atoms.

At all conditions, the inner capacitance values are large and increase with temperature (Fig. 6). For the tetradentate configuration utilizing the MUSIC model, C_1 values increase from 3.93 F · m^{-2} at 25°C to 6.52 F · m^{-2} at 250°C. Away from the pH_{zpc} these large C_1 values translate into an electrostatic contribution to Ca^{2+} adsorption that is at most (extremes of the pH range) 20% of the total adsorption free energy ($\Delta G^0_{intrinsic} + \Delta G^0_{electrostatic}$), at all temperatures. These large capacitance values also suggest that Ca^{2+} is bound to rutile in inner-sphere fashion, indicating a separation distance less than that of the hydrated ion radius. At higher temperatures capacitance values exceed those expected given the bare Ca^{2+} radius and a Stern layer dielectric constant equal to the corresponding bulk water value, which may indicate Ca^{2+} binding below the plane of average surface charge on the rutile surface. This is conceivable geometrically since Ca^{2+} is small enough to sink below the average surface oxygen plane as defined by the tetradentate adsorption site.

The fitted capacitance values can be related to the relative dielectric constant of the Stern layer (ε_s) according to (Hiemstra and van Riemsdijk, 1991; Stumm, 1992):

$$C = \varepsilon_0\varepsilon_s/d \quad (27)$$

where C is the inner capacitance value at the Ca^{2+} binding plane (in units of F · m^{-2}), and d is the distance of charge separation (in meters). If C is taken from the tetradentate

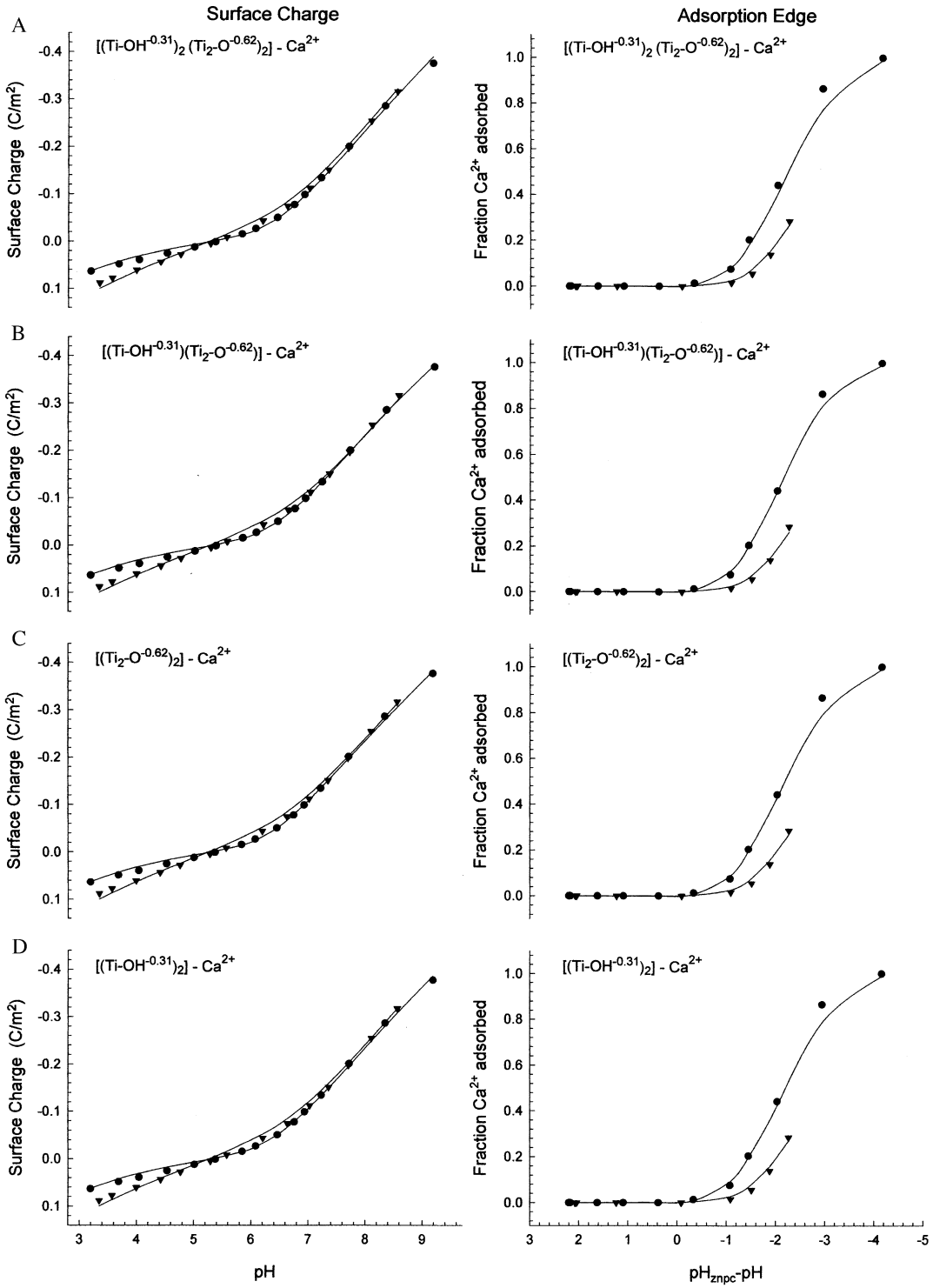

Fig. 5. Alternate surface complexes for the sorption of Ca^{2+} onto rutile at 25°C, at 0.03 (●) and 0.3-*m* (▼) (NaCl) ionic strength. All experimental data are shown as closed symbols, whereas the best-fit curves are shown as solid lines. In the left-hand column the proton charge versus pH data are shown, whereas the right-hand column provides the fits of adsorption 'pH-edge' data. In plots A to F the MUSIC model is used, with the following surface site geometries: (A) a tetradentate configuration; (B) a bidentate fit comprising one singly ($\equiv TiOH^{-0.31}$) and one doubly ($\equiv Ti_2O^{-0.62}$) coordinated surface groups; (C) a bidentate fit with two doubly coordinated surface groups; (D) a bidentate fit with two singly coordinated surface groups; (E) a monodentate fit with a doubly coordinate surface group; and (F) a monodentate fit with a singly coordinate surface group. Plot G shows a tetradentate configuration using the 1-p*K* model; whereas, plot H shows a tetradentate fit using the CD-MUSIC model with $f = 0.300$. All model parameter values are defined in the text and are given in Tables 1, 2, and 4.

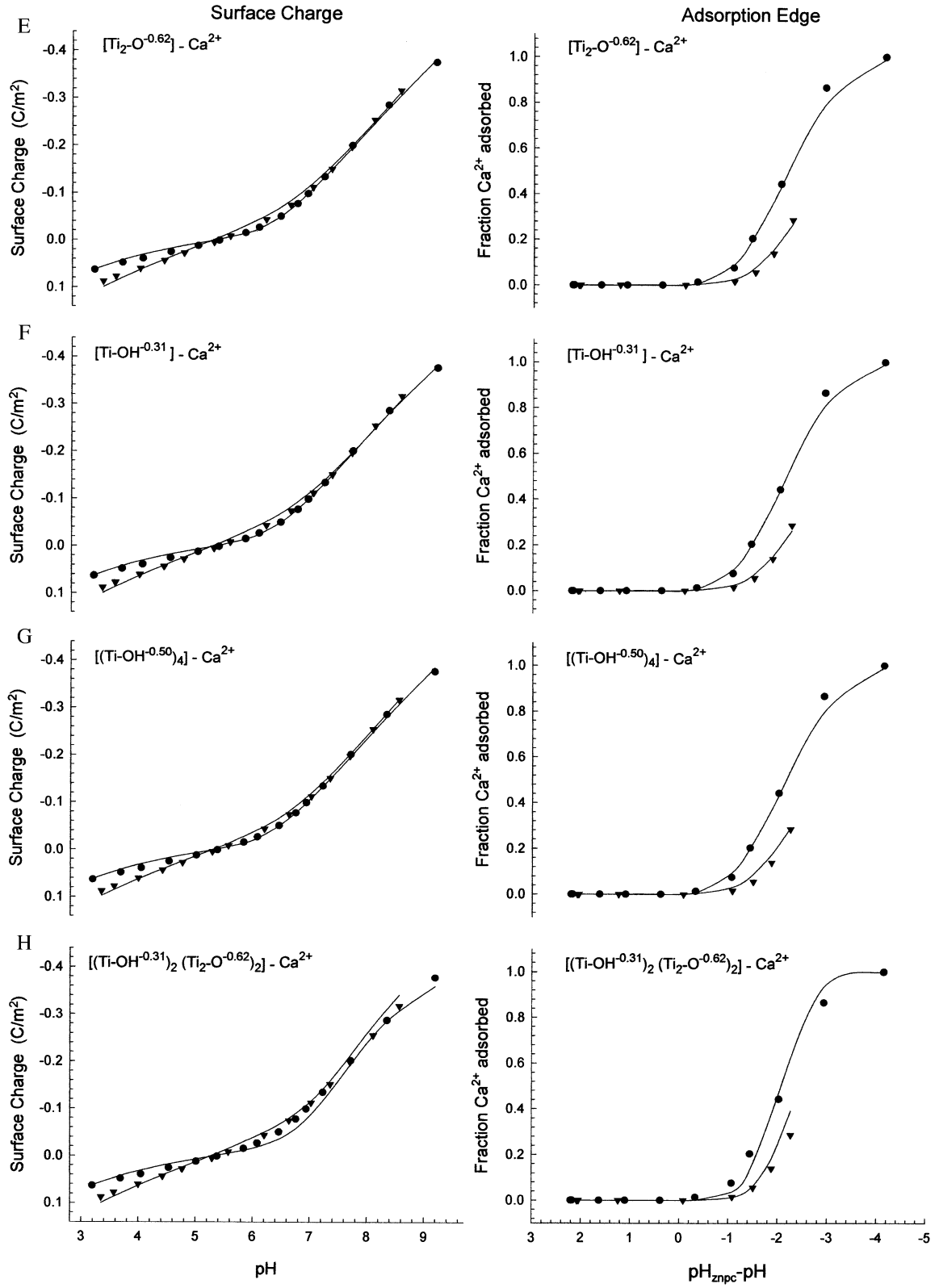

Fig. 5. Continued.

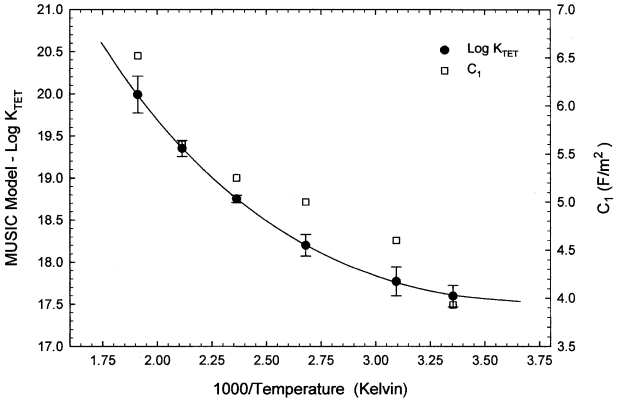

Fig. 6. Variation in logK_{TET} (binding constants for Ca^{2+} adsorbed to rutile in a tetradentate configuration) and C_1 as a function of 1/temperature in kelvins.

configuration/MUSIC model fit at 25°C ($C_1 = 3.93\ \mathrm{F \cdot m^{-2}}$), and d is taken from the X-ray standing wave measurements of Fenter et al. (2000) where $d_{\mathrm{Sr}} = 1.3$ Å, then the dielectric constant of the Stern layer may be estimated. The resulting value of ε_s at 25°C is 57.70, which is lower than the dielectric constant of the bulk solution ($\varepsilon_b = 78.45$ at 25°C). The reduction in the Stern layer dielectric constant suggests that the near-surface water is somewhat polarized as expected for a charged interface. At present, it is not possible to make similar estimates of ε_s at higher temperatures since corresponding X-ray standing wave measurements have not been made at elevated temperatures.

4.4. Surface Speciation

Surface site speciation and the associated distribution of charge between the various surface groups can be calculated using the parameter values in Tables 1 and 3. Figure 7 presents the results of these calculations at an intermediate temperature and ionic strength (150°C and 0.3 *m* with 0.001 *m* initial Ca^{2+}) of the conditions studied. Clearly, the fraction of individual surface species and change in surface charge are strongly pH dependent. In the example shown, and at all other conditions, the $TiOH_2^{+0.69}$ and $Ti_2O^{-0.62}$ species predominate over much of the experimental pH range. The fraction of surface sites associated with Na^+ and Cl^- counterions is always small, even at relatively high ionic strengths. However, a significant fraction of surface sites are associated with Ca^{2+} as pH increases above the pH_{znpc} value. The $[(=TiOH)_2(=Ti_2O)_2] - Ca$ species becomes one of the predominant species at high pH; whereas in the absence of Ca^{2+}, the fraction of $TiOH^{-0.31}$ and $Ti_2O^{-0.62}$ would increase.

In the lower plot of Figure 7, the contribution to charge of surface sites associated with the Na^+ and Cl^- counterions have been omitted for clarity. Except at very high ionic strength, these species contribute little to the overall charge in the presence of Ca^{2+} ion binding. For example, at the experimental conditions shown, the contribution to charge development from Na^+ surface species increases from -1.84×10^{-3} to $-0.0533\ \mathrm{C \cdot m^{-2}}$, whereas charge of the Cl^- surface species decreases from 0.0116 to $2.059 \times 10^{-4}\ \mathrm{C \cdot m^{-2}}$. At low pH (pH $<$ pH_{znpc}) the net surface charge is determined by changes in the speciation of protonated and unprotonated Ti-O surface sites, whereas above the pH_{znpc} net surface charge is determined predominantly from the charge contributed by the Ca^{2+} surface species. Also shown in Figure 7 is the total charge associated with both the Stern and diffuse layers. The Stern layer charge dominates above the pH_{znpc} with the major contribution from the inner Ca-binding plane.

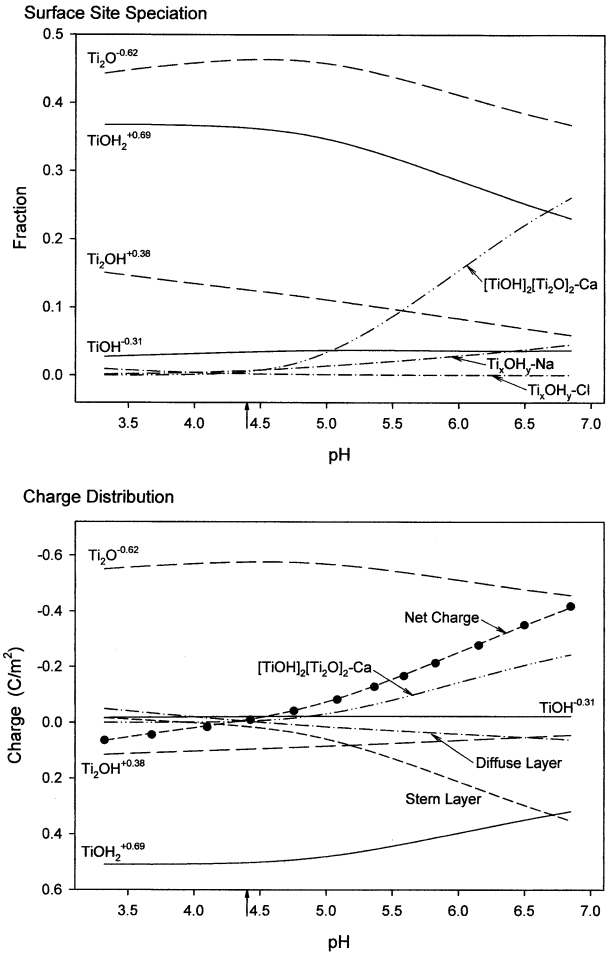

Fig. 7. Surface species distributions at 150°C and $I = 0.3$ *m* with 0.001-*m* initial Ca^{2+}. In the upper plot surface species are presented as fractions of the total concentration of surface sites, N_S, which was fixed at 20.8 $\mu\mathrm{mol \cdot m^{-2}}$. The lower plot shows the charge contribution of each surface species to the total proton induced surface charge. The arrow at pH 4.4 marks the pH_{znpc} value at 150°C.

5. CONCLUSIONS

Explicit consideration of a spectroscopically identified inner-sphere tetradentate adsorption complex, within the MUSIC model approach and a three plane Stern based description of EDL structure, successfully describes Ca^{2+} adsorption by rutile from 25 to 250°C. This is the first use of any surface complexation model to describe divalent cation adsorption well into the hydrothermal regime. Calcium adsorption increases with temperature and this is reflected by increases in both best-fit

tetradentate binding constants and associated inner Stern layer capacitance values. The increased capacitance values suggest that Ca^{2+} moves closer to the rutile surface with increasing temperature.

It is also demonstrated that several alternate mono- and bidentate adsorption complexes can adequately describe Ca^{2+} adsorption by rutile. This reinforces the concept that macroscopic data alone cannot distinguish between various adsorption mechanisms (e.g., Westall and Hohl, 1980; Sposito, 1986; Brown, 1990). Rather, it is necessary to combine information from both the molecular and macroscopic scale to provide unique mechanistically-accurate, thermodynamically-rigorous descriptions of ion adsorption phenomena at solid-solution interfaces.

Acknowledgments—This research was support by the National Science Foundation (EAR-0124001 and EAR-9627784). Additional support was provided by the Office of Basic Energy Sciences, U.S. Department of Energy, under contract #DE-AC05-00OR22725 with Oak Ridge National Laboratory, managed by UT-Battelle, LLC. MLM acknowledges the support of the Illinois State Water Survey and the Illinois Department of Natural Resources.

Associate editor: R. A. Wogelius

REFERENCES

Akaike H. (1976) An information criterion (AIC). *Math Sci.* **14,** 5–9.

Angrove M. J., Wells J. D., and Johnson B. B. (1999) The influence of temperature on the adsorption of cadmium(II) and cobalt(II) on goethite. *J. Colloid Interface Sci.* **211,** 281–290.

Archer D. G. and Wang P. (1990) The dielectric-constant of water and Debye-Huckel limiting law slopes. *J. Phys. Chem. Ref. Data* **19,** 371–411.

Axe L., Bunker G. B., Anderson P. R., and Tyson T. A. (1998) An XAFS analysis of strontium at the hydrous ferric oxide surface. *J. Colloid Interface Sci.* **199,** 44–52.

Bedzyk M. J. and Cheng L. (2002) X-ray standing wave studies of minerals and mineral surfaces: Principles and applications. In *Applications of Synchrotron Radiation in Low-Temperature Geochemistry and Environmental Science* (eds. P. A. Fenter, M. L. Rivers, N. C. Sturchio, and S. R. Sutton), chap. 4. Mineralogical Society of America, Washington, DC.

Boily J. F., Persson P., and Sjöberg S. (1999) *A Refined Multisite Complexation Model for Cd(II) Surface Complexes on Goethite Particles of Different Surface Areas*. Unpublished manuscript from the Ph.D. thesis of J. F. Boily, Department of Chemistry, Umeå University.

Bolt G. H. and van Reimsdijk W. H. (1982) Ion adsorption of inorganic variable charge constituents. In *Soil Chemistry Part B: Physico-Chemical Models* (ed. G. J. Bolt), pp. 459–804. Elsevier, New York.

Brown G. R. Jr. (1990) Spectroscopic studies of chemisorption reaction mechanisms at oxide/water interfaces. In *Mineral-Water Interface Geochemistry* (eds. M. F. Hochella and A. F. White), chap. 8. Mineralogical Society of America, Washington, DC.

Brown G. R. Jr., Parks G. A., Bargar J. R., and Towle S. N. (1999) Use of X-ray absorption spectroscopy to study reaction mechanisms at metal oxide-water interfaces. In *Mineral-Water Interfacial Reactions: Kinetics and Mechanisms.* ACS Symposium Series 715 (eds. D. L. Sparks and T. L. Grundl). chap. 2. American Chemical Society, Washington, DC.

Collins C. R., Sherman D. M., and Ragnarsdottir K. V. (1998) The adsorption mechanism of Sr^{2+} on the surface of goethite. *Radiochim. Acta* **81,** 201–206.

Criscenti L. J. and Sverjensky D. A. (1999) The role of electrolyte anions (ClO_4^-, NO_3^-, and Cl^-) in divalent metal (M^{2+}) adsorption on oxide and hydroxide surfaces in salt solutions. *Am. J. Sci.* **299,** 828–899.

Fenter P., Cheng L., Rihs S., Machesky M., Bedzyk M. J., and Sturchio N. C. (2000) Electrical double-layer structure at the rutile-water interface as observed *in situ* with small-period x-ray standing waves. *J. Colloid Interface Sci.* **225,** 154–165.

Gibb A. W. M. and Koopal L. K. (1990) Electochemistry of a model for patchwise heterogeneous surfaces: The rutile-hematite system. *J. Colloid Interface Sci.* **134,** 12–138.

Hayes K. F. and Katz L. E. (1996) Application of x-ray absorption spectroscopy for surface complexation modeling of metal ion adsorption. In *Physics and Chemistry of Mineral Surfaces* (ed. P. V. Brady), pp. 147–223. CRC Press, Boca Raton, FL.

Helgeson H. C., Kirkham D. H., and Flowers G. C. (1981) Theoretical prediction of the thermodynamic behavior of aqueous-electrolytes at high-pressures and temperatures. 4. Calculation of activity-coefficients, osmotic coefficients, and apparent molal and standard and relative partial molal properties to 600-degrees-C and 5 Kb. *Am. J. Sci.* **281,** 1249–1516.

Hiemstra T. and van Riemskijk W. H. (1991) Physical-chemical interpretation of primary charging behavior of metal (hydr)oxides. *Colloids Surf.* **59,** 7–25.

Hiemstra T. and van Riemskijk W. H. (1996) A surface structural approach to ion adsorption: The charge distribution (CD) model. *J. Colloid Interface Sci.* **179,** 488–508.

Hiemstra T., van Riemskijk W. H., and Bolt G. H. (1989) Multisite proton adsorption modeling at the solid/solution interface of (hydr)oxides: A new approach. *J. Colloid Interface Sci.* **133,** 91–104.

Hiemstra T., Venema P., and van Riemskijk W. H. (1996) Intrinsic proton affinity of reactive surface groups of metal (hydr)oxides: The bond valence principle. *J. Colloid Interface Sci.* **184,** 680–692.

Holmes H. F., Busey R. H., Simson J. M., and Mesmer R. E. (1994) $CaCl_{2(aq)}$ at elevated-temperatures—Enthalpies of dilution, isopiestic molalities, and thermodynamic properties. *J. Chem. Thermodynam.* **26,** 271–298.

James R. O. and Healy T. W. (1972) Adsorption of hydrolysable metal ions at the oxide-water interface. III. Thermodynamic model of adsorption. *J. Colloid Interface Sci.* **40,** 65–81.

Jones P. and Hockey J. A. (1971) Infra-red studies of rutile surfaces. 2. Hydroxylation, hydration, and structure of rutile surfaces. *Trans. Faraday Soc.* **67,** 2679–2685.

Karasyova O. N., Ivanova L. I., Lakshtanov L. Z., and Lovgren L. (1999) Strontium sorption on hematite at elevated temperatures. *J. Colloid Interface Sci.* **220,** 419–428.

Kulik D. A. (2000) Thermodynamic properties of surface species at the mineral-water interface under hydrothermal conditions: A Gibbs energy minimization single-site 2p*K*(A) triple-layer model of rutile in NaCl electrolyte to 250 degrees C. *Geochim. Cosmochim. Acta* **64,** 3161–3179.

Machesky M. L., Palmer D. A., and Wesolowski D. J. (1994) Hydrogen ion adsorption at the rutile-water interface to 250°C. *Geochim. Cosmochim. Acta* **58,** 5627–5632.

Machesky M. L., Wesolowski D. J., Palmer D. A., and Hayashi K.-I. (1998) Potentiometric titrations of rutile suspensions to 250°C. *J. Colloid Interface Sci.* **200,** 298–309.

Machesky M. L., Wesolowski D. J., Palmer D. A., and Ridley M. K. (2001) On the temperature dependence of intrinsic surface protonation equilibrium constants: An extension of the revised MUSIC model. *J. Colloid Interface Sci.* **239,** 314–327.

Marcus Y. (1995) *Ion properties*. Marcel Dekker, Inc, New York.

Mesmer R. E., Marshall W. L., Palmer D. A., Simonson J. M., and Holmes H. F. (1988) Thermodynamics of aqueous association and ionization reactions at high-temperatures and pressures. *J. Sol. Chem.* **17,** 699–718.

Meissner H. P. and Kusik C. L. (1972) Activity coefficients of strong electrolytes in Multicomponent aqueous solutions. *AIChE J.* **18,** 294–298.

Murray R. C. and Cobble J. W. (1980) Chemical equilibria in aqueous systems at high temperatures. In *Proceedings of the 41st International Water Conference*, pp. 1–82. Eng. Soc. Western PA.

Pitzer K. S., Peiper J. C., and Busey R. H. (1984) Thermodynamic properties of aqueous sodium-chloride solutions. *J. Phys. Chem. Ref. Data* **13,** 1–102.

Pivovarov S. (2001) Adsorption of cadmium onto hematite: Temperature dependence. *J. Colloid Interface Sci.* **234,** 1–8.

Ridley M. K., Machesky M. L., Wesolowski D. J., and Palmer D. A. (1999) Calcium adsorption at the rutile-water interface: A potentiometric study in NaCl media to 250°C. *Geochim. Cosmochim. Acta* **63,** 3087–3096.

Ridley M. K., Machesky M. L., Palmer D. A., and Wesolowski D. J. (2002a) Potentiometric studies of the rutile-water interface: Hydrogen-electrode concentration-cell vs glass-electrode titrations. *Colloids Surf. A: Physicochem. Eng. Aspects* **204,** 295–308.

Ridley M. K., Machesky M. L., Wesolowski D. J., and Palmer D. A. (2002b) Sorption of neodymium versus strontium on rutile surfaces to elevated temperatures. *Geol. Soc. Am. Abstr.* **34**.

Ridley M. K., Wesolowski D. J., Machesky M. L., Palmer D.A., Zhang Z., Fenter P., and Sturchio N. C. (2002c) Interaction of calcium and strontium at the rutile-water interface from 25 to 250°C. *American Chemical Society, Orlando, FL, USA, April 7-11, 2002*.

Rietra R. P. J. J., Hiemstra T., and van Riemsdijk W. H. (1999) Sulfate adsorption of goethite. *J. Colloid Interface Sci.* **218,** 511–521.

Rietra R. P. J. J., Hiemstra T., and van Riemsdijk W. H. (2001) Interaction between calcium and phosphate adsorption on goethite. *Environ. Sci. Technol.* **35,** 3369–3374.

Sahai N. (2000) Estimating adsorption enthalpies and affinity sequences of monovalent electrolyte ions on oxide surfaces in aqueous solution. *Geochim. Cosmochim. Acta* **64,** 3629–3641.

Sahai N., Carroll S. A., Roberts S., and O'Day P. A. (2000) X-ray absorption spectroscopy of strontium(II) coordination. II. Sorption and precipitation at kaolinite, amorphous silica and goethite surfaces. *J. Colloid Interface Sci.* **222,** 198–212.

Spadini L., Manceau A., Schindler P. W., and Charlet L. (1994) Structure and stability of Cd^{2+} surface complexes on ferric oxides. *J. Colloid Interface Sci.* **168,** 73–86.

Sposito G. (1986) Distinguishing adsorption from surface precipitation. In *Geochemical Processes at Mineral Surfaces* ACS Symposium Series 323 (eds. J. A. Davis and K. F. Hayes), pp. 217–228. American Chemical Society, Washington, DC.

Stumm W. (1992) *Chemistry of the Solid-Water Interface*. John Wiley, New York.

Sverjensky D. A. and Sahai N. (1998) Theoretical prediction of single-site enthalpies of surface protonation for oxides and silicates in water. *Geochim. Cosmochim. Acta* **62,** 3703–3716.

Towle S. N., Brown G .E. Jr., and Parks G. A. (1999a) Sorption of Co(II) on metal oxide surfaces. I. Identification of specific binding sites of Co(II) on (110) and (001) surfaces of TiO_2 (rutile) by grazing-incidence XAFS spectroscopy. *J. Colloid Interface Sci.* **217,** 299–311.

Towle S. N., Bargar J. R., Brown G. E. Jr., and Parks G. A. (1999b) Sorption of Co(II) on metal oxide surfaces. II. Identification of Co(II)(aq) adsorption sites on the (0001) and ($1\bar{1}02$) surfaces of α-Al_2O_3 by grazing-incidence XAFS spectroscopy. *J. Colloid Interface Sci.* **217,** 312–321.

Venema P., Hiemstra T., and van Riemskijk W. H. (1996) Multisite adsorption of cadmium on goethite. *J. Colloid Interface Sci.* **183,** 515–527.

Waychunas G. A. (2002) Grazing-incidence X-ray absorption and emission spectroscopy. In *Applications of Synchrotron Radiation in Low-Temperature Geochemistry and Environmental Science* (eds. P. A. Fenter, M. L. Rivers, N. C. Sturchio, and S. R. Sutton), chap. 5. Mineralogical Society of America, Washington, DC.

Westall J. and Hohl H. (1980) A comparison of electrostatic models for the oxide/solution interface. *Adv. Colloid Interface Sci.* **12,** 265–294.